

Aquaporin Positron Emission Tomography Differentiates Between Grade III and IV Human Astrocytoma

Yuji Suzuki, MD*

Yukihiro Nakamura, PhD*

Kenichi Yamada, MD*

Satoshi Kurabe, MD*†

Kouchirou Okamoto, MD*‡

Hiroshi Aoki, MD‡

Hiroki Kitaura, DDS* §

Akiyoshi Kakita, MD§

Yukihiko Fujii, MD‡

Vincent J. Huber, PhD*

Hironaka Igarashi, MD*‡

Ingrid L. Kwee, MD¶

Tsutomu Nakada, MD*

*Center for Integrated Human Brain Science, Brain Research Institute, University of Niigata, Niigata, Japan; †Department of Neurosurgery, Brain Research Institute, University of Niigata, Niigata, Japan; ‡Department of Pathology, Brain Research Institute, University of Niigata, Niigata, Japan; §Department of Neurology, University of California, Davis, California

Correspondence:

Yuji Suzuki, MD, PhD,
Center for Integrated Human Brain
Science,
Brain Research Institute,
University of Niigata,
1-757 Asahimachi,
Niigata 951-8585, Japan.
E-mail: yuji-s@bri.niigata-u.ac.jp

Received, July 29, 2016.

Accepted, May 15, 2017.

Published Online, June 21, 2017.

© Congress of Neurological Surgeons
2017.

This is an Open Access article distributed under the terms of the Creative Commons Attribution-NonCommercial-NoDerivs licence (<http://creativecommons.org/licenses/by-nc-nd/4.0/>), which permits non-commercial reproduction and distribution of the work, in any medium, provided the original work is not altered or transformed in any way, and that the work is properly cited. For commercial re-use, please contact journals.permissions@oup.com

BACKGROUND: Aquaporin (AQP) water channels play a significant role in mesenchymal microvascular proliferation and infiltrative growth. AQPs are highly expressed in malignant astrocytomas, and a positive correlation is observed between their expression levels and histological tumor grade.

OBJECTIVE: To examine the utility of aquaporin positron emission tomography (PET) for differentiating between astrocytoma grade III and grade IV using the AQP radioligand [¹¹C]TGN-020.

METHODS: Fifteen astrocytoma patients, grade III (n = 7) and grade IV (n = 8), and 10 healthy volunteers underwent [¹¹C]TGN-020 aquaporin PET imaging. Surgical tissues of astrocytoma patients were examined for histopathological grading using the WHO classification standard and expression of AQP1 and AQP4 immunohistochemically.

RESULTS: Mean standardized uptake values of astrocytoma grade III and IV (0.51 ± 0.11 vs 1.50 ± 0.44 , respectively) were higher than normal white matter (0.17 ± 0.02 , $P < .001$) for both tumor grades. Importantly, mean standardized uptake values of astrocytoma grade IV were significantly higher than grade III ($P < .01$).

CONCLUSION: Our study demonstrated that [¹¹C]TGN-020 aquaporin PET imaging differentiated between astrocytoma grades III and IV. We suggest its clinical application as a noninvasive diagnostic tool would lead to advancements in the management of these malignant brain tumors.

KEY WORDS Aquaporin1 (AQP1), Aquaporin4 (AQP4), Astrocytoma, [¹¹C]TGN-020, Positron emission tomography (PET)

Neurosurgery 82:842–846, 2018

DOI:10.1093/neuros/nyx314

www.neurosurgery-online.com

Aquaporins (AQPs) are ubiquitously expressed throughout the human body. AQP1 and AQP4 have an extremely regulated distribution in the central nervous system (CNS), where they play important roles in cerebrospinal fluid production and absorption and the regulation of blood-brain barrier water permeability. Recent studies have reported a relationship between astrocytoma malignancy and the abnormal expression of AQPs in the

CNS, particularly AQP1 and AQP4.^{1,2} These water channel proteins are highly expressed in malignant astrocytomas,^{3,4} and a positive correlation is observed between their expression levels and histological tumor grade.^{5,6} Both AQPs have significant roles in mesenchymal microvascular proliferation and infiltrative growth.⁶⁻¹⁰ Indeed, malignant astrocytoma is characterized by microvascular proliferation and diffuse, infiltrative growth, tumor characteristics that are believed to promote tumor progression and portend a poor prognosis. Therefore, the evaluation of both the AQPs' expression in malignant astrocytoma patients in vivo would lead to an early diagnosis of malignancy and an accurate evaluation of the extent of malignant tumor regions. However, real-time in vivo visualization of AQPs in brain tumor has not been reported previously.

ABBREVIATIONS: AQPs, Aquaporins; CNS, central nervous system; CT, computed tomography; IR, immunoreactivity; PET, positron emission tomography; SUV, standardized uptake value; 3D, three-dimensional

TGN-020 is an AQP ligand that uniquely binds to AQP1 and AQP4.^{11,12} Its radioligand, [¹¹C]TGN-020, has previously successfully demonstrated the distribution of AQP in normal human brain using positron emission tomography (PET).¹³ In this study, we evaluated the AQP1 and AQP4 distribution in astrocytoma patients using [¹¹C]TGN-020 PET imaging and, furthermore, considered the difference in ligand uptake between grade III and IV astrocytoma.

METHODS

Participants

Malignant astrocytoma patients were recruited between November 2012 and October 2015 in accordance with the human research guidelines of the local Internal Review Board. All patients underwent gross total resection surgeries within a week of PET imaging, and none were treated using steroids. Histopathologic tumor diagnosis was completed based on the surgical specimens. Of the 23 patients recruited into this study, 5 were excluded for other tumor diagnoses; 4 oligodendroglioma and 1 central neurocytoma. In addition, 3 diffuse astrocytoma (WHO grade II) patients were excluded from the statistical analysis due to the limited sample size. Finally, the remaining 15 high-grade astrocytoma patients (age 29–81 yr, 48.3 ± 14.5), grade III (4 males and 3 females) and grade IV (5 males and 3 females), and 10 healthy volunteers (age 24–85 yr, 46.2 ± 19.5 , 6 males and 4 females) participated in this study and were included in all statistical analyses. Written informed consent was obtained from each participant prior to the PET study. Informed consent included the description and intended use of [¹¹C]TGN-020, an unlabeled product. This trial was registered at the UMIN Clinical Trials Registry as UMIN000005626 (<http://www.umin.ac.jp/ctr/index.htm>).

[¹¹C]TGN-020 Synthesis

The radioligand, [¹¹C]TGN-020, was prepared using a TRACERlab FX_C Versatile Automated Synthesizer (GE Healthcare, Schenectady, New York) as previously detailed.^{13,14} Quality control measurements on all solutions for human injection consisted of pH, chemical purity, radiochemical purity, and endotoxin tests. All [¹¹C]TGN-020 samples used in this study had chemical and radiochemical purities > 95%, with radiochemical yields between 400 and 600 MBq.

PET Images

The [¹¹C]TGN-020 PET/computed tomography (CT) scan was acquired using a combination PET/CT scanner (Discovery ST Elite, GE Healthcare). Low-dose CT scans were performed in helical mode with 120 kVp, 50 mA, helical thickness of 3.75 mm, and 15 cm field of view positioned in the region of the cerebrum. [¹¹C]TGN-020 (160–272 MBq, 2.2–4.2 MBq/kg body weight) was administered intravenously in 2 min by syringe pump (PHD2000, Harvard, Cambridge, Massachusetts). PET emission data were acquired over 30 min in 3-dimensional (3D) statistic mode, from 10 min after the administration of [¹¹C]TGN-020, with a 25.6 cm axial field of view. The emission scans were reconstructed with a 128 × 128 × 47 matrix (a voxel size of 2.0 × 2.0 × 3.27 mm) using a 3D ordered subset expectation maximization iterative reconstruction algorithm (2 iterations and 28 subsets) after attenuation correction using the CT data. All PET images were transferred to a workstation Xeleris 3.1 (GE Healthcare) for analysis. Tissue activity concentration was expressed as the standardized uptake value

(SUV), g/ml, corrected for subject's body weight and administered dose of radioactivity.

Statistical Analysis

Three investigators, including a board-certified neuroradiologist and a board-certified neurosurgeon, drew the regions of interest (ROIs) using Volumetrix MI on a workstation Xeleris 3.1, in reference to tumor regions in the magnetic resonance imaging (MRI) images. We set an SUV 0.3 or more as the tumor-positive regions in the software. Comparison of mean SUVs between parietal white matter in normal volunteers and grade III and grade IV astrocytoma in patients, respectively, was performed using the Mann–Whitney *U*-test (2-tailed). *P* values of .01 or lower were considered to be statistically significant. Analyses were performed using IBM SPSS Statistics 22.0 (IBM Corporation, Armonk, New York). *P* values were corrected for multiple comparisons by Bonferroni method.

Histopathologic Tumor Grading and Immunohistochemistry

Surgical specimens taken from patients were fixed in 20% formalin, phosphate buffered. Tumor grading was assessed by histopathological examination of surgical tissue according to the WHO classification standard for diffuse astrocytoma grade III and grade IV. Immunohistochemistry was performed on paraffin-embedded, 4 μm thick sections with primary antibodies against AQP1 (monoclonal; ab168387, Abcam, Cambridge, United Kingdom) and AQP4 (polyclonal; gift from Dr Kenji Sakimura¹⁵). Reactivity was visualized using the avidin-biotin-peroxidase complex method (Vector, California). Diaminobenzidine was used as the chromogen. Immunoreactivity (IR) of both AQP1 and AQP4 in tumorous region were assessed semiquantitatively and scored on a 3-point scale (immunoreactivity score: 1, weak; 2, moderate; 3, intense). The 3-point scale assessments were performed by 2 neuropathologists. The scores were analyzed using the Mann–Whitney *U*-test (2-tailed), and *P* values of .05 or lower were considered to be statistically significant.

RESULTS

T2-weighted MRI and [¹¹C]TGN-020 PET images are shown in Figure 1. Scale bars (right side) indicate corresponding SUV (g/ml). Astrocytoma grades III and IV showed more intense qualitative intratumoral [¹¹C]TGN-020 uptake compared to normal white matter area. Furthermore, [¹¹C]TGN-020 uptake in astrocytoma grade IV was more intense than in grade III.

Mean SUVs for normal volunteer white matter and astrocytoma grades III and IV are presented quantitatively in Figure 2. Mean SUVs of astrocytoma grades III and IV (0.51 ± 0.11 and 1.50 ± 0.44 , respectively) were higher than that of normal white matter (0.17 ± 0.02 , $P < .001$) for both tumor grades. Importantly, mean SUVs of astrocytoma grade IV were significantly higher than those of grade III ($P < .01$).

Immunohistochemical expression of AQP1 and AQP4 was detected in all surgical specimens taken from patients with WHO astrocytoma classification grade III ($n = 7$) and grade IV ($n = 8$). AQP1 IR was observed in the cytoplasm and proximal processes of the tumor cells, whereas AQP4 IR was more conspicuous in cell processes and endfeet attaching to blood vessels. Semiquantified

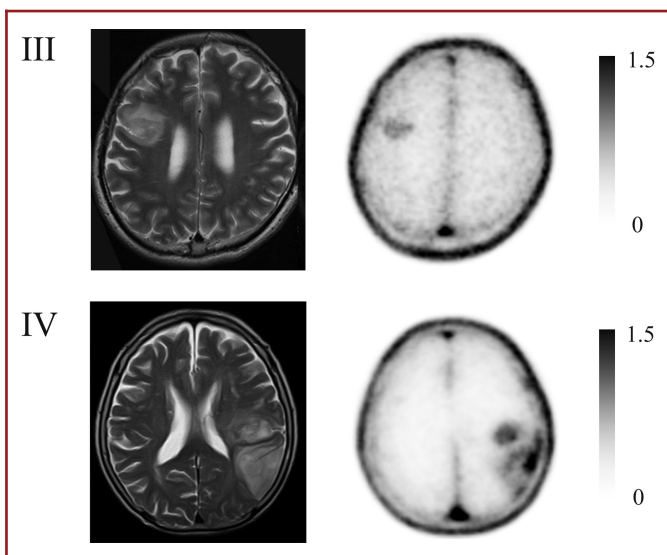


FIGURE 1. T2-weighted MRI and [^{11}C]TGN-020 PET images. T2-weighted MRI (left) and [^{11}C]TGN-020 PET (right) images of astrocytoma grade III (top) and grade IV (bottom) are shown. The scale bar indicating SUV (g/ml) is shown to the right of the corresponding PET image.

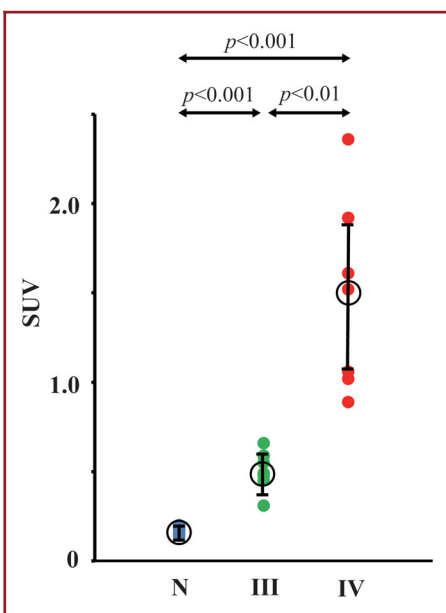


FIGURE 2. Individual and mean SUV and standard deviation are shown for each patient group. Individual (solid circles) and mean (open circles) SUV and standard deviation for [^{11}C]TGN-020 uptake in white matter of normal volunteers (N, blue) and astrocytoma grade III (III, green) and grade IV (IV, red) patients. P values from the Mann-Whitney U-test (2-tailed) are shown above the respective figure entries.

IR-scores of both AQP1 and AQP4, which were assessed on a 3-point scale (IR-score: 1, weak; 2, moderate; 3, intense), showed significant increases in grade IV compared to grade III (AQP1: 1.7 ± 0.49 vs 2.6 ± 0.53 , AQP4: 1.9 ± 0.69 vs 2.9 ± 0.38 , grade III vs grade IV, $P < .05$, respectively; Figure 3).

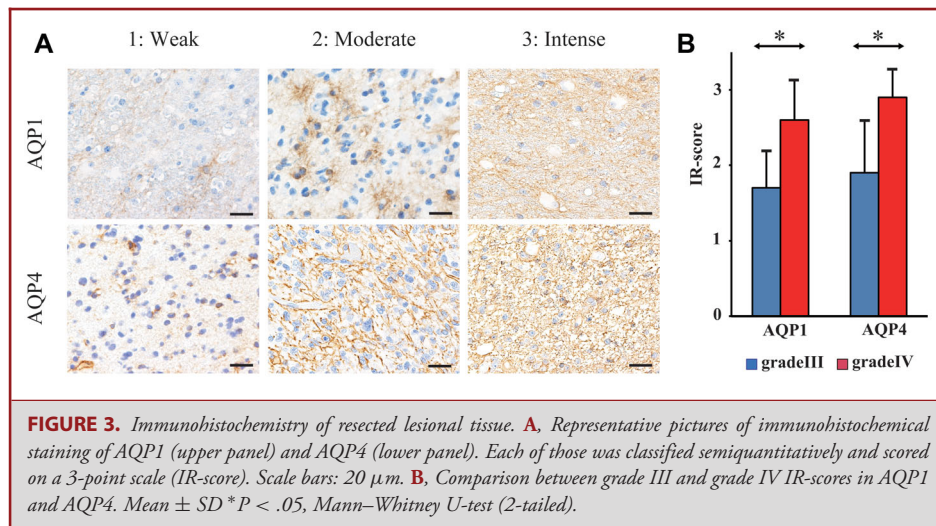
DISCUSSION

AQP1 is highly expressed along the vascular lumen in peripheral tissues. In the CNS, however, vascular AQP1 expression is completely suppressed. The normal distribution of AQP1 in the CNS is instead limited to choroid plexus epithelial cells.¹ Moreover, there is virtually no expression of AQP1 in healthy astrocytes. By contrast, AQP4 is widely expressed throughout the CNS, primarily along astrocyte endfeet membranes contacting the basal lamina surrounding capillaries and dura, as well as, secondarily, along the processes of astrocyte endfeet.²

In malignant astrocytoma grades III and IV, active suppression of vascular AQP1 is lost, leading to significant AQP1 expression in proliferating microvessels and clinically correlating to loss of blood-brain barrier integrity. Studies have shown that AQP1 expression in vessels enhance tumor cell migration.^{6,7} Indeed, a significant reduction in tumor growth and angiogenesis are found in AQP1-deficient mice.¹⁶ Increased AQP4 expression is also evident in astrocytoma cells, particularly when there is microvascular proliferation. Unlike normal AQP4 distribution on endfeet membranes contacting the basal lamina, astrocytoma AQP4 distribution is more uniform along endfeet membranes that are not in contact with the basal lamina.¹⁷ This altered AQP4 expression pattern appears to correlate with infiltration of tumor cells into surrounding healthy tissue.⁸⁻¹⁰ Alterations in AQP1 and AQP4 expression in malignant astrocytoma thus correlate with malignant properties, ie, tumor cell infiltration and angiogenesis. The latter is thought to be the result of epithelial-mesenchymal transition, histopathologically recognized as mesenchymal microvascular proliferation.^{18,19,20}

The current study demonstrated that astrocytoma grades III and IV had significantly higher uptake of the aquaporin PET ligand [^{11}C]TGN-020 relative to normal white matter, though the results are preliminary due to the small sample size. Importantly, uptake increase was proportional to tumor grade, clearly differentiating the 2 tumor grades. Immunohistochemical studies confirmed that astrocytoma grades III and IV were associated with a dramatic increase in AQP1 and AQP4 expression and distribution compared to normal tissue.

Clinically, the term malignant astrocytoma refers to highly aggressive tumor characterized by infiltration and mesenchymal microvasculature proliferation. Although most common malignant astrocytoma is glioblastoma multiforme (WHO grade IV), anaplastic astrocytoma (WHO grade III) may also be included. The results of this study demonstrated a clear



distinction between the 2 grades of malignant astrocytoma. However, it remains impossible to identify a clear grade III-IV cutoff value due to the small samples.

The study provides support for aquaporin PET as a noninvasive tool in differentiating between astrocytoma grade III and grade IV. However, as a matter of course, replication of this study involving a larger number of patients will be necessary to determine to what extent aquaporin PET can differentiate between astrocytoma grade III and IV. Furthermore, 3 astrocytoma grade II patients participated in this study but were excluded from the statistical analysis due to the limited sample size. However, the mean SUV of astrocytoma grade II (0.30 ± 0.02) was lower than that of other malignant astrocytomas but did not reach statistical significance, in part due to the small sample size. We understand the method for distinguishing low- and high-grade astrocytomas would be useful clinically. The median survival period for the most common malignant astrocytoma, glioblastoma multiforme, is less than 15 mo from diagnosis.²⁰ A reliable clinical diagnostic method that can provide information regarding tumor grade and extent of infiltration should translate to early treatment and surgical planning of patients. It is suggested that [¹¹C]TGN-020 PET would be regarded as one of the methods.

In addition to distinguishing between astrocytoma grades III and IV, the present PET study also suggests a therapeutic potential for AQP1 and AQP4 inhibitors in the treatment of astrocytoma grades III and IV. Given that proliferation, migration, and infiltration are major biological properties of malignant brain tumors and involve abnormal AQP distribution, AQP1 and AQP4 are considered potential drug targets for oncotherapy.^{12,21} Increased uptake of [¹¹C]TGN-020 in astrocytoma grades III and IV relative to surrounding healthy tissue may also suggest that selective AQP inhibitors will be helpful in arresting tumor growth and infiltration without damaging healthy tissue. Accordingly, we anticipate that further studies involving AQP imaging agents

and inhibitors would lead to the development of new therapeutic approaches.

CONCLUSION

Our study demonstrated that [¹¹C]TGN-020 aquaporin PET imaging differentiates between astrocytoma grades III and IV noninvasively. Its clinical application could help advance the management of these malignant brain tumors.

Disclosures

This study was supported by grants from the Ministry of Education, Culture, Sports, Science, and Technology (Japan) and University of Niigata. The authors have no personal, financial, or institutional interest in any of the drugs, materials, or devices described in this article.

REFERENCES

- Nielsen S, Nagelhus EA, Amiry-Moghaddam M, Bourque C, Agre P, Ottersen OP. Specialized membrane domains for water transport in glial cells: high-resolution immunogold cytochemistry of aquaporin-4 in rat brain. *J Neurosci.* 1997;17(1):171-180.
- Nielsen S, Smith BL, Christensen EI, Agre P. Distribution of the aquaporin CHIP in secretory and absorptive epithelia and capillary endothelia. *Proc Natl Acad Sci U S A.* 1993;90(15):7275-7279.
- Saadoun S, Papadopoulos MC, Davies DC, Bell BA, Krishna S. Increased aquaporin 1 water channel expression in human brain tumors. *Br J Cancer.* 2002;87(6):621-623.
- Saadoun S, Papadopoulos MC, Davies DC, Krishna S, Bell BA. Aquaporin-4 expression is increased in oedematous human brain tumours. *J Neurol Neurosurg Psychiatry.* 2002;72(2):262-265.
- Warth A, Kröger S, Wolburg H. Redistribution of aquaporin-4 in human glioblastoma correlates with loss of agrin immunoreactivity from brain capillary basal laminae. *Acta Neuropathol.* 2004;107(4):311-318.
- El Hindy N, Bankfalvi A, Herring A, et al. Correlation of aquaporin-1 water channel protein expression with tumor angiogenesis in human astrocytoma. *Anticancer Res.* 2013;33(2):609-613.
- McCoy E, Sontheimer H. Expression and function of water channels (aquaporins) in migrating malignant astrocytes. *Glia.* 2007;55(10):1034-1043.

8. McCoy ES, Haas BR, Sontheimer H. Water permeability through aquaporin-4 is regulated by protein kinase C and becomes rate-limiting for glioma invasion. *Neuroscience*. 2010;168(4):971-981.
9. Ding T, Ma Y, Li W, et al. Role of aquaporin-4 in the regulation of migration and invasion of human glioma cells. *Int J Oncol*. 2011;38(6):1521-1531.
10. Saadoun S, Papadopoulos MC, Watanabe H, Yan D, Manley GT, Verkman AS. Involvement of aquaporin-4 in astroglial cell migration and glial scar formation. *J Cell Sci*. 2005;118(pt 24):5691-5698.
11. Huber VJ, Tsujita M, Nakada T. Identification of aquaporin 4 inhibitors using in vitro and in silico methods. *Bioorg Med Chem*. 2009;17(1):411-417.
12. Huber VJ, Tsujita M, Nakada T. Aquaporins in drug discovery and pharmacotherapy. *Mol Aspects Med*. 2012;33(5-6):691-703.
13. Suzuki Y, Nakamura Y, Yamada K, Huber VJ, Tsujita M, Nakada T. Aquaporin-4 positron emission tomography imaging of the human brain: first report. *J Neuroimaging*. 2013;23(2):219-233.
14. Nakamura Y, Suzuki Y, Tsujita M, Huber VJ, Yamada K, Nakada T. Development of a novel ligand, [11C]TGN-020, for aquaporin 4 positron emission tomography imaging. *ACS Chem Neurosci*. 2011;2(10):568-571.
15. Tanaka K, Tani T, Tanaka M, et al. Anti-aquaporin 4 antibody in selected Japanese multiple sclerosis patients with long spinal cord lesions. *Mult Scler*. 2007;13(7):850-855.
16. Saadoun S, Papadopoulos MC, Hara-Chikuma M, Verkman AS. Impairment of angiogenesis and cell migration by targeted aquaporin-1 gene disruption. *Nature*. 2005;434(7034):786-792.
17. Noell S, Wolburg-Buchholz K, Mack AF, et al. Dynamics of expression patterns of AQP4, dystroglycan, agrin and matrix metalloproteinases in human glioblastoma. *Cell Tissue Res*. 2012;347(2):429-441.
18. Brat DJ. Astrocytic tumors. In: Love S, Budka H, Ironside JW, Perry A, eds. *Greenfield's Neuropathology*, 9th ed. Boca Raton: CRC Press; 2015:1638-1672.
19. Milson CC, Yu JL, Mackman N, et al. Tissue factor regulation by epidermal growth factor receptor and epithelial-to-mesenchymal transitions: effect on tumor initiation and angiogenesis. *Cancer Res*. 2008;68(24):10068-10076.
20. Stupp R, Mason WP, van den Bent MJ, et al. Radiotherapy plus concomitant and adjuvant temozolomide for glioblastoma. *N Engl J Med*. 2005;352(10):987-996.
21. Yool AJ, Brown EA, Flynn GA. Roles for novel pharmacological blockers of aquaporins in the treatment of brain oedema and cancer. *Clin Exp Pharmacol Physiol*. 2010;37(4):403-409.

Acknowledgment

The authors are very grateful to Mr Yuta Yagi for his help in PET ligand synthesis and PET image acquisition.

COMMENTS

In this article, the authors report preliminary findings regarding the ability of a novel molecular imaging technique, [¹¹C] TGN-020 PET, to distinguish between grade III and grade IV malignant astrocytomas. TGN-020 is an aquaporin ligand that binds uniquely to AQP1 and AQP4, aquaporin proteins, which have recently been shown to be expressed in high levels in malignant astrocytomas. In a small cohort of 15 patients with high-grade astrocytomas (grades III and IV), the authors found that the tumors demonstrated a significantly higher mean standard uptake value (SUV) compared to normal white matter on [¹¹C] TGN-020 PET and also, perhaps more importantly, that grade IV astrocytomas showed a significantly higher mean SUV than grade III astrocytomas. In addition, the authors were able to demonstrate significant differences in the immunohistochemical expression of both AQP1 and AQP4 between grade III and grade IV gliomas.

These findings suggest that [¹¹C] TGN-020 PET could be a valuable diagnostic and prognostic tool for patients with primary brain tumors. Unfortunately, due to the constraints of the study, which was limited

to a very small sample of grade III and IV gliomas, conclusions based on these results cannot be generalized beyond patients with high-grade tumors. In addition, although [¹¹C] TGN-020 PET appears in this study to have been excellent at discriminating grade III and grade IV gliomas, it is reasonable to wonder how the technique stacks up for noninvasive tumor grading against other promising and widely available MR based techniques, such as diffusion kurtosis imaging, dynamic contrast enhanced permeability imaging, and susceptibility weighted imaging (just to name a few). Ultimately, it remains to be seen whether and how [¹¹C] TGN-020 PET will be used in clinical practice in the future.

It is also unfortunate that the authors did not incorporate genetic data on the tumors in this study in their analysis, particularly in light of what we now know about how IDH mutation status predicts clinical behavior in patients with glioblastoma. Nevertheless, [¹¹C] TGN-020 PET appears to be an exciting new tool in neuro-oncologic imaging, and the findings in this study open the door to a number of avenues for future investigation, including studies on the potential value of aquaporin imaging for furthering our understanding glioma biology and pathogenesis, noninvasive tumor grading, prognosis determination, clinical management, and development of new therapeutic targets.

Benjamin Huang

Chapel Hill, North Carolina

The authors studied the role of [¹¹C] TGN-020 aquaporin PET imaging in the evaluation of malignant gliomas. TGN-020 is an aquaporin ligand that selectively binds to Aquaporin 1 (AQP1) and Aquaporin 4 (AQP4), water channel proteins highly expressed in malignant astrocytomas.¹ Interestingly, AQP1 is expressed by choroid plexus epithelial cells, but not by normal astrocytes.² On the other hand, AQP4 has greater expression in malignant glioma cells than healthy astrocytes.³ This study shows promising differences in the uptake of TGN-020 between grade III and grade IV astrocytomas, although the small size of the sample (n = 15) limits the potential impact of the current study results. Future studies should build upon these preliminary observations. The next step will be to validate the differences in uptake between grade III and IV astrocytomas in larger cohorts. Furthermore, the role of [¹¹C] TGN-020 aquaporin PET imaging in the characterization of low-grade gliomas and early identification of anaplastic transformation of grade II gliomas should be further investigated. Further development of aquaporin imaging agents and inhibitors may lead to the development of novel therapeutic approaches for astrocytic tumors.⁴ In the future AQP1 and AQP4 may serve as potential drug targets for neuro-oncology treatments.

Maria Vittoria Spampinato

Charleston, South Carolina

1. Isokpehi RD, Wollenberg Valero KC, Graham BE, et al. Secondary data analytics of aquaporin expression levels in glioblastoma stem-like cells. *Cancer Inform*. 2015;14:95-103.
2. Johansson PA, Dziegielewska KM, Ek CJ et al. Aquaporin-1 in the choroid plexuses of developing mammalian brain. *Cell Tissue Res*. 2005; 322(3):353-364.
3. Iacovetta C, Rudloff E, Kirby R. The role of aquaporin 4 in the brain. *Vet Clin Pathol*. 2012;41(1):32-44.
4. Verkman AS, Anderson MO, Papadopoulos MC. Aquaporins: important but elusive drug targets. *Nat Rev Drug Discov*. 2014;13(4):259-277.